

Evidence for a magnetic-polaron state in the low-carrier system CeP

M. Kohgi and T. Osakabe

Department of Physics, Tohoku University, Sendai 980, Japan

K. Kakurai

Institute for Solid State Physics, University of Tokyo, Roppongi, Tokyo 106, Japan

T. Suzuki, Y. Haga, and T. Kasuya

Department of Physics, Tohoku University, Sendai 980, Japan

(Received 14 January 1994)

Elastic neutron-scattering experiments performed in the low-carrier system CeP show interesting magnetic diffraction patterns under a magnetic field. They can be explained by the stacking of the ferromagnetically coupled Γ_8 double Ce layers among the antiferromagnetically coupled Γ_7 layers with a period of eleven Ce layers along the field direction, even though the crystal-field level energy of Γ_8 is 160 K. The result gives direct evidence for the existence of the magnetic-polaron state in CeP proposed by Kasuya *et al.*

Strongly correlated low-carrier-density systems are now attracting much attention, in particular in connection to the high- T_c materials. In this sense, CeSb with the NaCl-type crystal structure is a prototypical material belonging to this class of materials. Trivalent rare-earth mononictides are compensated semimetals with low-carrier density and, different from the doped systems, essentially intrinsic character can be extracted by using pure samples. CeSb is a typical low-carrier Kondo-lattice system, contradicting the usual impurity Kondo picture. Furthermore, it exhibits a most complicated magnetic phase diagram, including a type of Devil's staircase at low temperatures.¹ Under an applied magnetic field, the so-called *FP* phases appear; in these phases, the ferromagnetic layer of the fully polarized $4f\Gamma_8$ state with the moment value of $2\mu_B$ stacks in various sequence among the Γ_7 layers. In the paramagnetic phase, however, the Γ_8 quartet is 35 K above the ground Γ_7 doublet. These anomalous properties were explained by Takahashi *et al.*² as the result of a strong *p-f*-mixing interaction with the Γ_8 -type holes of the valence band located at the Γ point of the Brillouin zone; the effect of this is strongly nonlinear because of the low hole concentration. The conduction band has a minimum at the *X* points and mixes very weakly with the $4f$ electrons.

Recently, very-high-quality single crystals of CeP were successfully prepared and it was shown that the carrier concentration in the material is much smaller than that in CeSb; it is of the order of 0.001/Ce at low temperatures, determined directly by the Shubnikov-de Haas (SdH) effect,³ and various anomalies were found in the transport and magnetic properties.³⁻⁶ They are rather similar to those of CeSb, although the ground-state properties are mainly due to the $4f\Gamma_7$ state and the crystal-field splitting is much larger (160 K) in the paramagnetic state.⁷ Such anomalies were not observed previously in

less pure CeP samples. Similar properties were also observed for very pure CeAs samples.^{4,8}

Kasuya *et al.* explained these anomalies based on the magnetic polaron model.⁹ It is well known that, in the limit of low-carrier concentration, the carrier system should behave as a Wigner crystal if the crystal is sufficiently pure. Because of its strong quantum-crystal character, the Wigner crystal melts easily and, in the usual concentration under consideration, it is thought to exist as a liquid state; this is called a Wigner liquid hereafter. In a magnetic system such as CeP, each quasilocalized hole polarizes the $4f\Gamma_8$ states through a strong Γ_8 *p-f*-mixing interaction, stabilizes the Wigner liquid, and changes it to a magnetic-polaron liquid. This state exists even at room temperature, and becomes stronger with decreasing temperature because of the increasing susceptibility of the $4f\Gamma_8$ state. It becomes rapidly weaker, however, when the temperature drops beyond the crystal-field splitting energy because the population of the Γ_8 state decreases. At low temperatures, in particular under an applied magnetic field, the entropy term in the free energy becomes unimportant, and this weak magnetic polaron changes to a strong magnetic polaron with a small radius and with a nearly saturated $4f\Gamma_8$ moment. Since the strong magnetic polaron cannot move easily due to its large effective mass, it exhibits magnetic order, preferring a ferromagnetic layered structure due to its strong intralayer *p-f* mixing. Various anomalous properties are explained by the above characteristics of a magnetic polaron. Formation of magnetic polarons was claimed to be a common feature of the strongly correlated low-carrier-density systems.

The magnetization process of the high-quality CeP sample obtained from the same batch as that for the present neutron-scattering experiment is shown in Fig. 1 for fields up to $H = 10$ T at 4.2 K, is well below the Néel

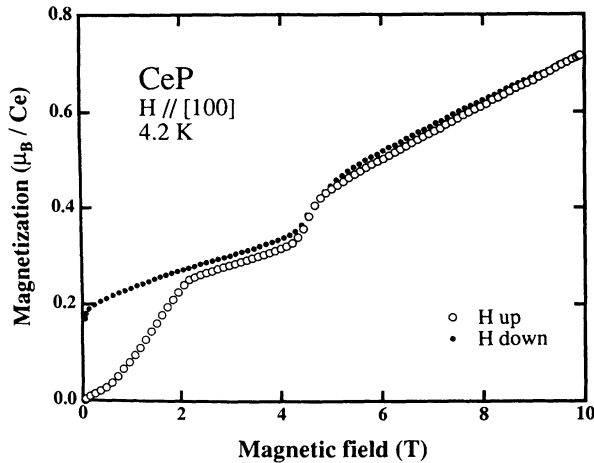


FIG. 1. Magnetization of CeP at 4.2 K for the field along $[0,0,1]$. The open and closed circles indicate the data with increasing and decreasing magnetic field, respectively.

temperature of $T_N = 10.5$ K. It is seen that there exist two different phases of the magnetic structure in this field range. Magnetization measurements for higher fields⁵ show that there is a kink at about 12 T, above which the magnetization increases much more slowly with many small steps. Interestingly, the field values for the steps align with equal spacing in $1/H$ scale, and the period coincides with that observed by the SdH experiment at lower fields.¹⁰ This suggests a strong correlation between magnetic order and the Fermi surface in CeP. The magnetization finally reaches the saturation value of Ce^{3+} ($2.1\mu_B$) after a rather large jump at 60 T. The magnetization at zero field extrapolated from the slope above 12 T gives the value for $4f\Gamma_7$ of $0.7\mu_B$. Based on these results, the authors of Ref. 5 claimed that the magnetization process of CeP up to 12 T corresponds to the canning process of the antiferromagnetic $4f\Gamma_7$ moments, the slower increase from 12 to 60 T is due to the mixing of the excited Γ_8 state to the Γ_7 ground state by the applied field, and the step at 60 T is due to the crossover to the Γ_8 originating state with a nearly full moment. The origin of the two-step increases of the magnetization below 5 T was, however, an open question.

In order to solve the above dispute, a detailed elastic neutron-scattering measurement has been performed on the 5G spectrometer (PONTA) at the JRR-3M reactor in JAERI by using a single crystal of CeP under magnetic field.

The sample was inserted in a horizontal Helmholtz-type superconducting magnet with the $[1, -1, 0]$ axis vertical. The magnetic field up to 6 T was applied along the $[0,0,1]$ axis. Thus the present experiment covers the two phases from $H = 2$ to 4 T and above 5 T in Fig. 1. Hereafter, they are referred to as phases I and II, respectively. The measurements were carried out mainly along $[2,2,\xi]$ and $[3,3,\xi]$ directions with ξ from 1.8 to 3.8. Figure 2 summarizes the obtained magnetic scattering patterns at $H = 0$, 2.7 T (phase I), and 5.5 T (phase II) at 5 K for $q = (0,0,\xi)$ in the reduced zone scheme. The data around $(2,2,2)$ and $(2,2,3)$ in the $[2,2,2+\xi]$ scans are not shown

in the figures because of strong nuclear scattering background from the sample or cryostat. The data in the figures are corrected for the background, magnetic form factor, Lorentz factor and angle factor in the magnetic scattering length. Here, the magnetic form factor of the Ce ion obtained by the dipole approximation¹² is employed. The direction of the magnetic moment is supposed to be parallel to the $[0,0,1]$ direction since no magnetic scattering was observed in the $(0,0,\xi)$ scan around $(0,0,1)$ at $H = 0$ and 5.5 T and, although weak magnetic intensities are seen at $H = 2.7$ T in the $(0,0,\xi)$ scan, they are only about $1/100$ of those around $(3,3,2)$ after the correction of the form factor and the Lorentz factor. Thus the patterns in the figures directly correspond to the square of the Fourier transform, $|F(\mathbf{q})|^2$, where $F(\mathbf{q}) = \sum_j \mu_j \exp(i\mathbf{q} \cdot \mathbf{r}_j) / N$, μ_j is the magnetic moment of atom at site j and N is the number of atoms in the sum.

The pattern at the zero-field state corresponds to that of the type-I antiferromagnetic ordering, where each ferromagnetically ordered $(0,0,1)$ plane stacks antiferromagnetically with the direction of the magnetic moment perpendicular to the plane. The magnetic moment per Ce atom is estimated to be $0.8 \pm 0.1\mu_B$ from the ratio of the integrated intensity of the $(3,3,2)$ peak to that of the $(3,3,3)$ nuclear peak at 5 K assuming the equivalent domain distribution. The results are consistent with the previous report for an impure sample.¹¹ Kasuya claimed that even without applied field some Γ_8 layers exist with replacing the Γ_7 layers. A somewhat larger antiferromagnetic moment, $0.8\mu_B$, than that of $4f\Gamma_7$ state may be

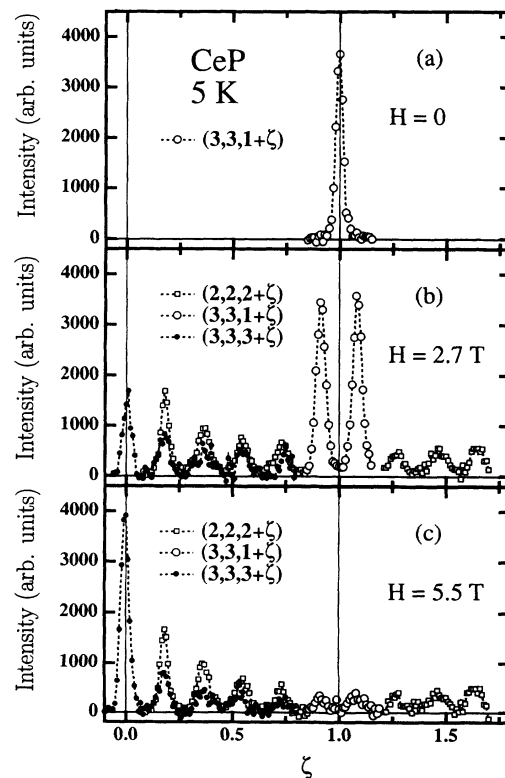


FIG. 2. Scattering patterns of CeP at 5 K at (a) zero field, (b) $H = 2.7$ T, and (c) $H = 5.5$ T in a reduced zone scheme.

due to this Γ_8 contribution, but more accurate measurement is needed to confirm this point.

The scattering patterns observed above 2 T are very striking. At $H=2.7$ and 5.5 T, the antiferromagnetic peak ($\zeta=1$) disappears and, instead, an array of peaks including the ferromagnetic component ($\zeta=0$) is seen. The ferromagnetic moments are estimated to be 0.24 ± 0.05 and $0.50\pm 0.10\mu_B$ per Ce atom at $H=2.7$ and 5.5 T, respectively. These values agree with the magnetization measurement shown in Fig. 1 within experimental errors. The positions of the satellite peaks seen at $H=2.7$ and 5.5 T are the same and given by multiples of the wave vector $(2\pi/a)\delta$, where a is the lattice parameter and $\delta=0.182\cong 2/11$. The corresponding magnetic structure is the layered structure with the fundamental period of eleven $(0,0,1)$ layers. At $H=2.7$ T, the fifth higher-order peak has the strongest intensity. However, at $H=5.5$ T, it almost disappears. Actually, when its intensity is traced continuously with increasing field, it increases in the same way as the increase of the magnetization, and decreases suddenly at about 5 T where the second stepwise increase of the magnetization is seen. On the other hand, the intensities of other higher-order peaks keep essentially the same values as those at $H=2.7$ T up to fields of 6 T. It should be noticed that there is a discrepancy of the satellite peak intensities between the $(2,2,2+\zeta)$ and $(3,3,3+\zeta)$ scans although both scans are considered to be equivalent for magnetic scattering. This point will be discussed later.

The observed scattering patterns in phase I can be reproduced well by the following ordering. The majority Ce atoms have the Γ_7 moment of about $0.7\mu_B$, and order antiferromagnetically as in the case of zero field. This order is cut just in the eleven layers period by the ferromagnetically coupled double layers with the moment value of about $2\mu_B$ per Ce in each layer. Hereafter, the large moment layers are regarded as the Γ_8 layers since their moment value is close to that of the Γ_8 state in CeSb. The Γ_7 moment on the nearest-neighbor layer of the Γ_8 double layer couples antiferromagnetically with the Γ_8 moment. Therefore, the Γ_7 order shows the antiphase domain structure. This is the origin of the strong fifth higher-order peak. The order of the Γ_8 double layers mainly contributes to the observed ferromagnetic moment and to the strong satellite peaks other than the fifth. The disappearance of the fifth peak and the sudden increase of the ferromagnetic component in phase II can be explained by the disappearance of the antiferromagnetic stacking of the Γ_7 layers along the $[0,0,1]$ direction and, instead, having the ferromagnetic component of about $0.2\mu_B$ per Ce ion along the applied field. This does not necessarily mean the disappearance of the antiferromagnetic ordering in the Γ_7 layers in phase II since, within our present experimental condition, only the magnetic stacking along the $[0,0,1]$ direction can be detected. More extended study is now planned. It is important to notice that, in spite of the change in the Γ_7 layers, the order of the Γ_8 double layers never changes as seen clearly in the persistent satellite structure up to the fourth order.

To obtain a best fit to the observed scattering patterns, however, some modification to the above ideal structure

is necessary. The main origin for the modification seems to stem from a stacking fault for the Γ_8 double layer. Actually, the observed widths of the satellite peaks are about 30% broader than those of the $(3,3,2)$ peak at $H=0$ and $(3,3,3)$ peak above about 2 T, indicating that the order is not perfect but with a correlation range of 50–60 Å. There are, however, too many possible ways of the stacking fault and it is difficult to obtain a unique way of the modification. The results shown in Figs. 3 are obtained by the following physical conditions. By the stacking faults, the occupation of the Γ_8 double layers at the 0th and 1st sites decrease by about 19% from the perfect occupation, while about 4% of Γ_7 layers at the 2nd and 3rd as well as the 9th and 10th sites in both phases are replaced by the ferromagnetic Γ_8 double layers. In phase II, the additional ferromagnetic component on the 2nd and 10th sites is canceled by some induced antiferromagnetic components due to the antiferromagnetic interaction with the neighboring Γ_8 moment. Figures 4(a) and 4(b) show the integrated intensities of the observed peaks at 2.7 and 5.5 T together with the calculated results based on the proposed model shown in Figs. 3(a) and 3(b), respectively. The zero-field results are also shown in Fig. 4(a). The observed integrated intensities are put on an absolute scale of $|F(\mathbf{q})|^2$ by normalizing the ferromagnetic component at $H=5.5$ T to the value obtained from the magnetization.

Although the above assumptions are rather simple, the calculated results agree very well even in an absolute scale with the observed values for the $(3,3,3+\zeta)$ scan at both magnetic fields except for the fourth peak in phase I and the fifth peak in phase II. These discrepancies seem due to some modulation of the antiphase structure of the $4f\Gamma_7$ layers, which is neglected in the present consideration because we are mostly interested in the order of the Γ_8 layers. On the other hand, the systematic deviation of the intensity for the $(2,2,2+\zeta)$ scan from that of the $(3,3,3+\zeta)$ scan is more serious because such a deviation cannot be allowed in any magnetic ordering in the present crystal structure. Therefore, we are forced to assume that it comes from the contribution of nuclear scattering caused by the lattice distortion associated with the magnetic structure proposed above. One can show that about 1% distortion of the lattice spacing at the Γ_8 double layers gives nearly the same scattering as those of the magnetic scattering in the $(2,2,2+\zeta)$ scan. This gives

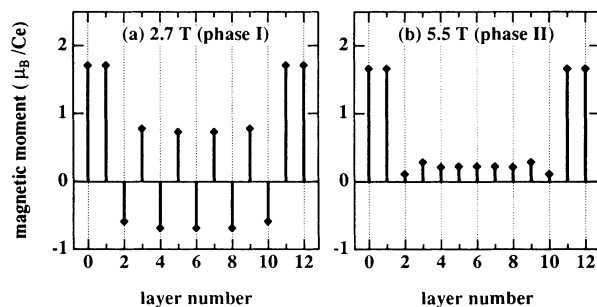


FIG. 3. Proposed model of the magnetic structure of CeP at (a) $H=2.7$ T (phase I) and (b) $H=5.5$ T (phase II).

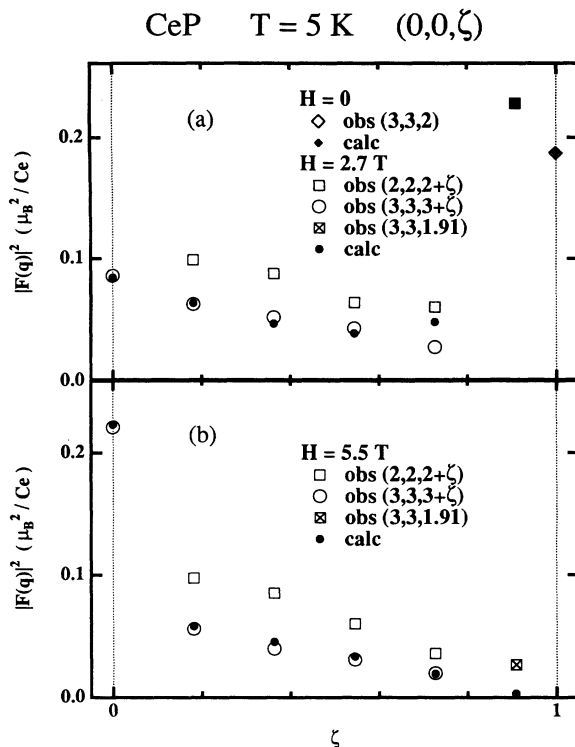


FIG. 4. Observed (open marks) and calculated (close marks) square of the Fourier component of the magnetic structure, $|F(\mathbf{q})|^2$, of CeP at 5 K, at (a) zero field and $H=2.7$ T, and (b) $H=5.5$ T.

no effect to the data in the $(3,3,3+\zeta)$ scan because of the negligibly small structure factor. For CeSb, a shrinking of the order of 10^{-3} was reported for the Γ_8 interlayer distance compared with that for the Γ_7 layers.¹³ In this respect, a 1% distortion seems to be a little too large even

though the p - f mixing is stronger in CeP than in CeSb. It is an urgent task to confirm this point.

To conclude, it is now clear that the stacking of the double ferromagnetic layers with a large Ce moment corresponding to the full polarization of $4f\Gamma_8$ state with the eleven layers period among the $4f\Gamma_7$ layers is realized in CeP under magnetic field. The results are consistent with the model proposed by Kasuya based on the magnetic-polaron picture. Any simple model which expects the mixing of the excited Γ_8 state by external or internal magnetic field cannot explain the present result because the applied field of about 2–5 T or the exchange field of the order of 10 K is too small to overcome the crystal field splitting of 160 K in CeP.¹⁴ The single Γ_8 layer model does not work because it is difficult to explain the observed antiphase domain structure. The double layers structure is also consistent with the *FP* phase in CeSb.

Finally the persistence of eleven layers period is considered in relation to the Fermi surface. The SdH oscillation observed for CeP shows the existence of a Fermi surface with an extremal cross section of 0.02 \AA^{-2} .¹⁰ Supposing that the Fermi surface is a sphere, the Fermi wave vector is estimated to be about $k_F \approx 0.08 \text{ \AA}^{-1}$. Interestingly, the observed fundamental wave vector $(2\pi/a)\delta$ of the magnetic order is quite close to twice that: $(2\pi/a)\delta = 0.19 \text{ \AA}^{-1}$. This fact strongly suggests that the ordering of the Γ_8 layers in CeP under magnetic field is realized by Fermi surface nesting. It must be also strongly correlated with the anomalous multistep magnetization process observed at high magnetic fields in CeP described before. A more detailed theoretical discussion concerning the present results is given in a separate paper.¹⁵

We thank M. Date, K. Sugiyama, and K. Kindo for useful discussions and communications. This work was partly supported by the Iketani Science and Technology Foundation.

¹See, for example, J. Rossat-mignod, J. M. Effantin, P. Burllet, T. Chattopadhyay, L. P. Regnault, H. Baltholin, O. Vogt, and D. Ravot, *J. Magn. Magn. Mater.* **52**, 111 (1985).

²See, for example, H. Takahashi and T. Kasuya, *J. Phys. C* **18**, 2697 (1985); **18**, 2709 (1985); **18**, 2721 (1985); **18**, 2731 (1985); **18**, 2745 (1985); **18**, 2755 (1985).

³Y. S. Kwon, Y. Haga, O. Nakamura, T. Suzuki, and T. Kasuya, *Physica B* **171**, 324 (1990).

⁴T. Suzuki, *Physical Properties of Actinide and Rare Earth Compounds* [Jpn. J. Appl. Phys. **8**, 268 (1993)].

⁵T. Kuroda, K. Sugiyama, Y. Haga, T. Suzuki, A. Yamagishi, and M. Date, *Physica B* **186-188**, 396 (1983).

⁶N. Môri, Y. Okayama, H. Takahashi, Y. Haga, and T. Suzuki, *Physical Properties of Actinide and Rare Earth Compounds* (Ref. 4), p. 182.

⁷M. Kohgi, Y. Osakabe, N. Môri, H. Takahashi, Y. Okayama,

H. Yoshizawa, Y. Ohara, S. Ikeda, T. Suzuki, and Y. Haga, *Physica B* **186-188**, 393 (1993).

⁸Y. S. Kwon, Y. Haga, S. Ozeki, T. Suzuki, and T. Kasuya, *Physica B* **169**, 497 (1991).

⁹T. Kasuya, Y. Haga, K. S. Kwon, and T. Suzuki, *Physica B* **186-188**, 9 (1993); T. Kasuya, T. Suzuki and Y. Haga, *J. Phys. Soc. Jpn.* **62**, 2549 (1993).

¹⁰Y. S. Kwon, thesis, Fac. Sci., Tohoku University, 1991.

¹¹H. Heer, A. Furrer, W. Hälgl, and O. Vogt, *J. Phys. C* **12**, 5207 (1979).

¹²C. Stassis, W. Deckman, B. N. Harmon, J. P. Desclaux, and A. J. Freeman, *Phys. Rev. B* **15**, 369 (1977).

¹³M. Sera, T. Suzuki, and T. Kasuya (unpublished).

¹⁴Y.-L. Wang and B. R. Cooper, *Phys. Rev. B* **2**, 2607 (1970).

¹⁵T. Kasuya, Y. Haga, T. Suzuki, T. Osakabe, and M. Kohgi, *J. Phys. Soc. Jpn.* **62**, 3376 (1993).